CHIN. PHYS. LETT. Vol. 37, No. 4 (2020) 048501

Analogue Soliton with Variable Mass in Super-Conducting Quantum Interference Devices *

Ying Yang(杨颖)[1], Ze-Hua Tian(田泽华)[2], Ji-Liang Jing(荆继良)[1]**

[1]*Department of Physics, Key Laboratory of Low Dimensional Quantum Structures and Quantum Control of Ministry of Education, and Synergetic Innovation Center for Quantum Effects and Applications, Hunan Normal University, Changsha 410081*

[2]*CAS Key Laboratory of Microscale Magnetic Resonance and Department of Modern Physics, University of Science and Technology of China, Hefei 230026*

(Received 19 November 2019)

It is difficult to investigate the behavior of solitons in realistic inhomogeneity media in experiment due to inhomogeneity of the media and noise from the unwanted coupling. We propose to use a waveguide-like transmission line which is based on direct-current super-conducting quantum interference devices to simulate behavior of solitons because we find that the behavior of the node flux in this transmission is similar to that of solitons with variable mass.

PACS: 85.25.Dq, 84.40.Az, 05.45.Yv, 52.35.Sb

DOI: 10.1088/0256-307X/37/4/048501

The sine-Gordon solitons have received considerable attention in many areas, such as one-dimensional crystal dislocation theory,[1−3] fluxon dynamics in Josephson transition line,[4,5] excitation of phonon modes,[6] condensation of charge density waves,[7,8] and DNA-promoter dynamics.[9−11]

In the standard sine-Gordon model, the solitons move with constant velocity and shape, while they may exhibit more complex motion with changing shape in realistic situations due to the inhomogeneity of the media.[12,13] In particular, inhomogeneity can lead to sine-Gordon solitons with variable mass which may be used as a desirable effect for fast transportation, fast communication, or even for a possible soliton gun.[14] However, it is difficult to investigate solitons in realistic inhomogeneous media in experiment because solitons in these media may exhibit more complex motion with changing velocity and shape, and the noise from unwanted coupling would also affect the detection. Therefore, it is interesting to find a way to simulate behavior of solitons in realistic inhomogeneous systems.

A promising candidate may be the current circuit quantum electrodynamics (cQED) technology which could offer a natural arena for testing behavior of solitons due to its fantastic controllability and scalability.[15] The development of super-conducting quantum interference device (SQUID) technology has been greatly promoted in many areas.[16−20] A lot of theoretical proposals for analog circuit realizations including Hawking radiation,[21] traversable wormhole spacetime,[22] Fermion–Fermion scattering in quantum field theory,[23] and dynamical gauge fields,[24,25] have been studied. Moreover, experimentally, the dynamic Casimir effect has been observed in a coplanar waveguide terminated by a SQUID[26] and in a Josephson material.[27] These studies open a new way to construct an experimental platform for research on many promising subjects.[15,28−33]

Based on the cQED technology, SQUIDs are a direction of great fundamental research. The operation of SQUIDs is based on interference between Cooper pairs passing through two different arms that comprise the interferometer loop. The external magnetic flux threading the loop is controllable, which determines the Josephson super-current carried by the device.

Due to the great significance of research for behavior of solitons in inhomogeneous media, we propose to use a super-conducting electrical circuit configuration which is based on micro-fabricated wave-guide and SQUIDs to simulate behavior of solitons with variable mass, and then discuss its experimental feasibility with current cQED technology.

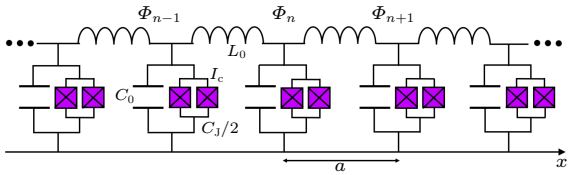

Fig. 1. Circuit diagram for a coplanar waveguide-like transmission line. The inductance for each inductor and the capacitance for each capacitor are assumed to be L_0 and C_0, respectively. Each SQUID element consists of two identical tunnel Josephson junctions, and the critical current is I_c, the capacitance is $C_J/2$. The length of all the cells is the constant a. The circuit is characterized by the dynamical fluxes Φ_n.

Now we consider a circuit model which is based on coplanar transmission line.[34,35] It is shown in Fig. 1 that each capacitor is parallel with the SQUID which consists of two parallel identical Josephson junctions (JJs) with the critical current I_c and capacitance $C_J/2$. Here we assume that the geometric size of the SQUID loop is so small that the SQUID self-inductance can be negligible contrasted to its kinetic inductance. Under this condition, we consider the single JJ with effective junction capacitance C_J and tunable Josephson energy $E_J(\Phi_{ext}^J) =$

*Supported by the National Natural Science Foundation of China under Grant Nos. 11875025, 11475061, and 11675052, and the CAS Key Laboratory for Research in Galaxies and Cosmology, Chinese Academy of Sciences under Grant No. 18010203.

**Corresponding author. Email: jljing@hunnu.edu.cn

© 2020 Chinese Physical Society and IOP Publishing Ltd

$2E_{\rm J}|\cos(\pi\Phi^{\rm J}_{\rm ext}/\Phi_0)|$,[34] where $\Phi^{\rm J}_{\rm ext}=BA_{\rm S}$ is the flux dropping through the SQUID loop with effective area $A_{\rm S}$ and the applied magnetic field B, $\Phi_0=h/2e$ is the magnetic flux quantum, and $E_{\rm J}$ is the Josephson energy expressed as $E_{\rm J}=\Phi_0 I_{\rm c}/(2\pi)$.

Two important energy scales determine the quantum mechanical behavior of a Josephson junction circuit: the Josephson coupling energy $E_{\rm J}$ and the electrostatic Coulomb energy $E_{\rm C}$ for a single Cooper pair, and the charging energy for a Cooper pair $E_{\rm C}=(2e)^2/2C_{\rm J}$.[36] Generally, there are several kinds of super-conducting qubits realized in different regimes of $E_{\rm J}/E_{\rm C}$.[37] The charge qubit is in the charge regime $E_{\rm C}\gg E_{\rm J}(\Phi^{\rm J}_{\rm ext})$, where the number n of Cooper pairs is well defined and the phase fluctuates strongly. The so-called flux and phase qubits are both in the phase regime $E_{\rm J}(\Phi^{\rm J}_{\rm ext})\gg E_{\rm C}$, in which the phase is well defined and n fluctuates strongly. The charge-flux qubit lies in the intermediate regime $E_{\rm J}(\Phi^{\rm J}_{\rm ext})\sim E_{\rm C}$, in which charge and phase degrees of freedom play equally important roles. Compared with the charge qubits, phase bits have longer decoherence time, so we restrict ourselves to the macroscopic SQUID junctions in this regime. In an SQUID array, the impedance comes not only from the electromagnetic environment (typically negligible), but also from the circuit elements and the transmission lines of the array, which lead to damping of the electric energy. In addition, the array is also influenced by thermal noise or quantum noise, which can cause the decoherence of the circuit.[38] Actually, the dissipation on an SQUID array is unavoidable in practice, and the effects are complex. In order to give an analytical result, we have to ignore some dissipation.

For this SQUID array, we can obtain the corresponding circuit Lagrangian of the system as follows:

$$\mathcal{L}=\sum_{n=1}^{N}\Big[\frac{1}{2}C_0\big(\dot{\Phi}_{\rm n}\big)^2-\frac{(\Phi_{n+1}-\Phi_{\rm n})^2}{2L_0}+\frac{1}{2}C_{\rm J}\big(\dot{\Phi}_{\rm n}\big)^2+E_{\rm J}(\Phi^{\rm J}_{\rm ext})\cos\Big(2\pi\frac{\Phi_{\rm n}}{\Phi_0}\Big)\Big],\tag{1}$$

where $\Phi_{\rm n}$ is the node flux. In the circuit, the frequencies is far less than the plasma frequency of the SQUID. The SQUID is operated in the phase regime where $E_{\rm J}(\Phi^{\rm J}_{\rm ext})\gg(2e)^2/2C_{\rm J}$. We assume that the wavelength λ for the flux is much longer than the dimensions of a single unit cell of the chain, i.e., $(a/\lambda\ll 1)$. In addition, we replace the discrete n by a continuous position x along the line, and substitute the finite difference in the Lagrangian by their continuous counterparts to first order in (a/λ), i.e., $\Phi_{\rm n}-\Phi_{n-1}\approx a\frac{\partial\Phi}{\partial x}+o(a^2)$. Therefore, the Lagrangian in Eq. (1) can be rewritten as

$$\mathcal{L}=\frac{C}{2}\int dx\Big[\Big(\frac{\partial\Phi}{\partial t}\Big)^2-\frac{a^2}{L_0C}\Big(\frac{\partial\Phi}{\partial x}\Big)^2+\frac{2E_{\rm J}(\Phi^{\rm J}_{\rm ext})}{C}\cos\Big(\frac{2\pi\Phi}{\Phi_0}\Big)\Big],\tag{2}$$

with $C=C_0+C_{\rm J}$. By taking $\phi=2\pi\Phi/\Phi_0$, we obtain the motion equation of the node flux ϕ through variation

$$\frac{\partial^2\phi}{\partial t^2}-\frac{a^2}{L_0C}\frac{\partial^2\phi}{\partial x^2}+\frac{1}{L_{\rm J}C}\sin\phi=0,\tag{3}$$

where $L_{\rm J}=\Phi_0/(4\pi^2E_{\rm J}(\Phi^{\rm J}_{\rm ext}))$ is the kinetic inductance of the equivalent single JJ. The last term in Eq. (3) is from the SQUID which provides a potential energy in Lagrangian (2) for the oscillator system. It is controllable because we can adjust the external magnetic flux $\Phi^{\rm J}_{\rm ext}$ by threading the SQUID loop to control the inductance $L_{\rm J}$.

Meanwhile, for a (1+1)-dimensional variable mass soliton, the sine-Gordon equation can be written as

$$\frac{\partial^2\phi}{\partial t^2}-c^2\frac{\partial^2\phi}{\partial x^2}+m^2\sin\phi=0.\tag{4}$$

Comparing Eq. (3) with Eq. (4), we find that they are very similar. The factor $a^2/(L_0C)$ in Eq. (3) is a constant, which corresponds to the coefficient c^2 on the second term in Eq. (4). The factor $1/(L_{\rm J}C)$ in Eq. (3) corresponds to m^2 in Eq. (4), which is the mass of the soliton. By appropriately adjusting the external magnetic flux $\Phi^{\rm J}_{\rm ext}$ through the SQUID loop, we can control $L_{\rm J}$ to simulate the soliton with different masses. Thus, simulating the dynamics of soliton with variable mass could be implemented in our setup.

We devote to utilize the above SQUID circuit to simulate the solitons with variable mass. To obtain the effect of various inhomogeneities on the soliton behavior, we consider some concrete integrable cases with variable mass, and analogue solitons in superconducting circuits with controllable conditions.

(i) Analogue soliton with mass $m=\frac{m_0}{l^2}(x^2-t^2)$. To realize the proposed experiment, an additional conducting line is needed to produce the space and time varying external flux bias $\Phi^{\rm J}_{\rm ext}$, which is used to modulate the SQUIDs for providing a potential energy. More specifically, we take

$$\Phi^{\rm J}_{\rm ext}=\frac{\Phi_0}{\pi}\arccos\Big[\frac{\Phi_0\,Cm_0^2(x^2-t^2)^2}{4\pi I_{\rm c}l^4}\Big],\tag{5}$$

and choose the relevant parameters for each element according to the references.[26,27,34,39,40] We assume the critical current $I_{\rm c}=10\,\mu$A, and capacitance $C_{\rm J}=0.3\,$fF for the JJ. The capacitance to ground is fixed as $C_0=0.1\,$fF, the inductance and the length of the single unit cell of our setup are assumed to be $L_0=0.004\,$nH and $a=12\,\mu$m, respectively. Then the behavior of the node flux is shown in Fig. 2. We observe that there is an intriguing flattening of the node flux at the center, which is the same as the analytic soliton with mass $m=m_0(x^2-t^2)$ in Ref. [13].

In Fig. 2, the intriguing change in the soliton shape during its motion is clearly. This required magnetic flux can be achieved by the corresponding current through the bias line.

Position dependent mass can be achieved in this case at $t\to 0$, and the dynamics of the soliton is shown in Fig. 3. Short time interval limit of the above soliton shows the flattening prominently. Here the relevant parameters for each element are similar to the above case.

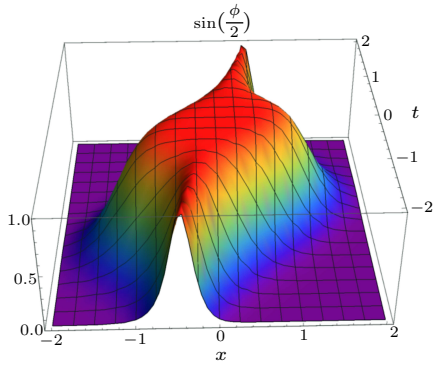

Fig. 2. Soliton with variable mass $m = \frac{m_0}{l^2}(x^2 - t^2)$. Here we assume the critical current $I_c = 10\,\mu A$, and capacitance $C_J = 0.3\,fF$ for the JJ. The capacitance to ground is fixed as $C_0 = 0.1\,fF$, and the inductance and the length of the single unit cell of our setup are assumed to be $L_0 = 0.004\,nH$ and $a = 12\,\mu m$, respectively. Here we choose $\frac{m_0}{l^2} = 1$.

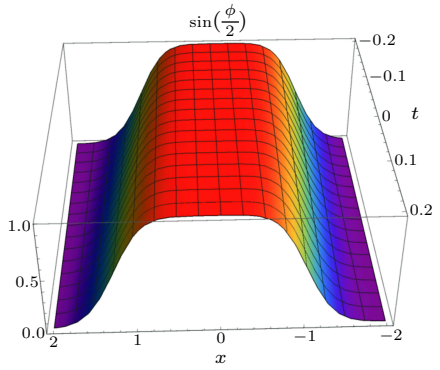

Fig. 3. Soliton with variable mass $m = \frac{m_0}{l^2}(x^2 - t^2)$ within short time interval limit. We assume the critical current $I_c = 10\,\mu A$, and capacitance $C_J = 0.3\,fF$ for the JJ. The capacitance to ground is fixed as $C_0 = 0.1\,fF$, and the inductance and the length of the single unit cell of our setup are assumed to be $L_0 = 0.004\,nH$ and $a = 12\,\mu m$, respectively. Here we choose $\frac{m_0}{l^2} = 1$.

(ii) Analogue soliton with mass $m = 2m_0 \cos q(x \pm t)$. The flux on propagation through JJ with the above soliton can be expressed as

$$\Phi_{ext}^{J} = \frac{\Phi_0}{\pi} \arccos\left[\frac{\Phi_0\, C m_0^2 \cos q^2 (x+t)^2}{\pi I_c}\right]. \tag{6}$$

We assume the critical current $I_c = 10\,\mu A$, and capacitance $C_J = 0.3\,fF$ for the JJ. The capacitance to ground is fixed as $C_0 = 0.1\,fF$, the inductance and the length of the single unit cell of our setup are assumed to be $L_0 = 0.004\,nH$ and $a = 12\,\mu m$, respectively. The oscillatory behavior of the node flux in the circuit is clearly seen in Fig. 4, which is similar to the analytic soliton with mass $m = 2m_0 \cos q(x \pm t)$ in Ref. [13].

(iii) Analogue soliton with mass $m = m_0(2\cos q(x+t)\cos q(x-t))^{\alpha/2}$. Soliton at short time interval limit ($t \to 0$) gives $m(x) \approx \tilde{m}_0(\cos qx)^{\alpha}$. A physically motivated spin chain with coupling constant changing periodically in space can be described by the variable mass soliton model with mass $m(x) = m_0(\cos qx)^{\alpha}$, where $\alpha = 1/(2-K)$, with $K \geq 1/2$ being an important parameter of the system.[12,41] For $\alpha = 1$ and $q = 1$, we obtain $\Phi_{ext}^{J} = (\Phi_0/\pi)\arccos(\Phi_0\, C m_0^2 \cos^2 x/(\pi I_c))$. We choose the critical current $I_c = 10\,\mu A$, and capacitance $C_J = 0.3\,fF$ for the JJ. The capacitance to ground is fixed at $C_0 = 0.1\,fF$, the inductance and the length of the single unit cell of our setup are assumed to be $L_0 = 0.004\,nH$ and $a = 12\,\mu m$, respectively. As shown in the left panel of Fig. 5, the soliton oscillates with space.

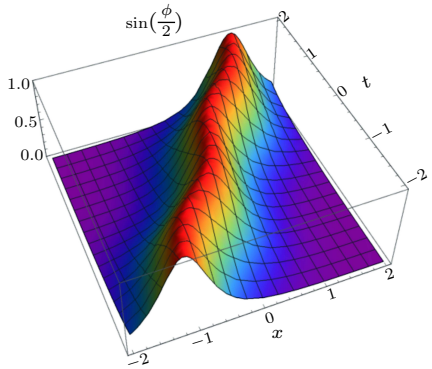

Fig. 4. Soliton with variable mass $m = 2m_0 \cos q(x+t)$. Here we assume the critical current $I_c = 10\,\mu A$, and capacitance $C_J = 0.3\,fF$ for the JJ. The capacitance to ground is fixed as $C_0 = 0.1\,fF$, the inductance and the length of the single unit cell of our setup are assumed to be $L_0 = 0.004\,nH$ and $a = 12\,\mu m$, respectively. Here, we choose $q = 1$ and $m_0 = 1$.

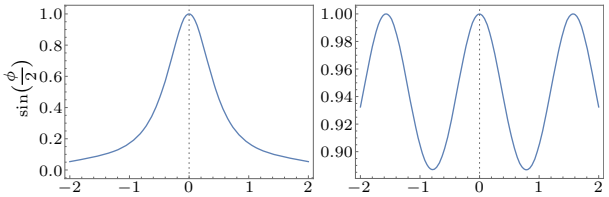

Fig. 5. Soliton with variable mass $m = 2m_0 \cos qx$ for left panel, and $m = 2m_0 \cos qt$ for the right panel. We assume the critical current $I_c = 10\,\mu A$, and capacitance $C_J = 0.3\,fF$ for the JJ. The capacitance to ground is fixed as $C_0 = 0.1\,fF$, the inductance and the length of the single unit cell of our setup are assumed to be $L_0 = 0.004\,nH$ and $a = 12\,\mu m$, respectively. Here we choose $m_0 = 1$ and $q = 1$.

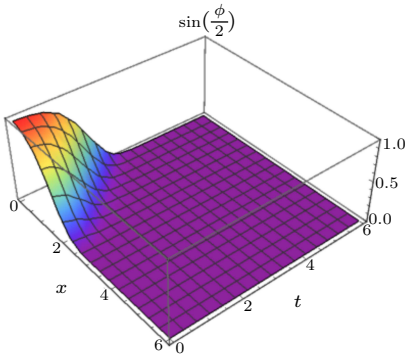

Fig. 6. Soliton with variable mass $m(x) = m_0 e^{\rho(x-x_0)}$. We assume the critical current $I_c = 10\,\mu A$, and capacitance $C_J = 0.3\,fF$ for the JJ. The capacitance to ground is fixed as $C_0 = 0.1\,fF$, the inductance and the length of the single unit cell of our setup are assumed to be $L_0 = 0.004\,nH$ and $a = 12\,\mu m$, respectively. Here we choose $\rho = 1.2$, $m_0 = 1$, and $x_0 = 1$.

Similarly, for a small space interval ($x \to 0$): $m(t) \approx \tilde{m}_0(\cos qt)^{\alpha}$, we obtain $\Phi_{ext}^{J} = (\Phi_0/\pi)\arccos(\Phi_0\, C m_0^2 \cos^2 t/(\pi I_c))$ for $\alpha = 1$ and

$q = 1$. Here the relevant parameters for each element is similar to the short time interval limit case. As shown in the right panel of Fig. 5, the node flux oscillates with time. A real oscillator chain is pumped by an alternating current,[42,43] which can be linked to a variable mass soliton with $m(t) = (\cos qt)^{1/2}$, and it can be used to describe the inhomogeneous spin wave dynamics[12] or evolution of the forced oscillators.[42,43]

(iv) Analogue soliton with mass $m = m_0 e^{\rho(x-x_0)}$ with $\rho = \text{const}$. Now we explore to simulate the soliton with only position-dependent mass $m(x)$. The flux on propagation through JJ with the above soliton can be expressed as

$$\Phi_{\text{ext}}^{\text{J}} = \frac{\Phi_0}{\pi} \arccos\left[\frac{\Phi_0 C m_0^2 \exp[2\rho(x-x_0)]}{\pi I_{\text{c}}}\right]. \quad (7)$$

We assume the critical current $I_{\text{c}} = 10\,\mu\text{A}$, and capacitance $C_{\text{J}} = 0.3\,\text{fF}$ for the JJ. The capacitance to ground is fixed as $C_0 = 0.1\,\text{fF}$, the inductance and the length of the single unit cell of our setup are assumed to be $L_0 = 0.004\,\text{nH}$ and $a = 12\,\text{nm}$, respectively. As shown in Fig. 6, we observe that the soliton shape changes. At $\rho \to 0$, the standard sine-Gordon soliton is recovered.

We have discussed the dynamics of the soliton by using the SQUID circuit. Such exact solitons show intriguing motion with changing shape, amplitude and width. However, for other cases, we could use this circuit to simulate the solitons by changing the flux on propagation through JJ, and then we can find the behavior of solitons by analyzing the output images of the circuit.

Due to the inhomogeneity of the media and noise from the unwanted coupling, solitons exhibit more complex motion with changing shape and direction. Therefore, it is difficult to investigate the behavior of solitons in realistic inhomogeneity media in experiment. We propose to use the SQUID circuit to simulate the behavior of solitons with variable mass because we can adjust the external magnetic flux $\Phi_{\text{ext}}^{\text{J}}$ threading the SQUID loop to control the inductance L_{J}, which is related to the mass of the soliton. We have simulated the following four kinds of solitons: (i) For the soliton with mass $m = m_0(x^2 - t^2)$, the output figure shows that there is an intriguing flattening at the center. For the short time-interval limit, this soliton shows the flattening prominently. (ii) For the soliton with mass $m = 2m_0 \cos^{\alpha} q(x \pm t)$, it oscillates periodically in spacetime. (iii) For the soliton with mass $m = m_0(2\cos q(x+t)\cos q(x-t))^{\alpha/2}$, which at the short time-interval limit ($t \to 0$) gives $m(x) \approx \tilde{m}_0(\cos qx)^{\alpha}$, and the soliton oscillates regularly. Similarly, for small space interval limit ($x \to 0$), soliton oscillates regularly along time. (iv) For the soliton with mass $m = m_0 e^{\rho(x-x_0)}$, it changes abruptly. It is noted that the transmission line could effectively reduce the noise from the unwanted coupling and make the detection of the soliton more effectively, then the illustration about the realistic inhomogeneous systems will become more clear. The parameters and pulse shapes in our study are chosen as an example that our setup is feasible, which should not be considered as the only available configuration. In fact, it is possible to improve and to optimize these values in terms of both the performance and fabrication of this proposal.

References

[1] Kochendörfer A and Seeger A 1950 *Z. Phys.* **127** 533
[2] Seeger A and Kochendörfer A 1951 *Z. Phys.* **130** 321
[3] Seeger A, Donth H and Kochendürfer A 1953 *Z. Phys.* **134** 173
[4] Scott A C 1970 *Il Nuovo Cimento B* **69** 241
[5] McLaughlin D W and Scott A C 1978 *Phys. Rev. A* **18** 1652
[6] Quintero N R and Kevrekidis P G 2001 *Phys. Rev. E* **64** 056608
[7] Baryakhtar V G 1994 *Dynamics of Topological Magnetic Solitons* (Berlin: Springer)
Remoissenet M 2003 *Waves Called Solitons* (Berlin: Springer)
Ludu A 2007 *Nonlinear Waves and Solitons on Contours and Closed Surfaces* (Berlin: Springer)
[8] Goldobin E et al 2004 *Phys. Rev. Lett.* **92** 057005
[9] Yakushevich L V et al 2002 *Phys. Rev. E* **66** 016614
[10] Bernardini A E et al 2015 *Eur. Phys. J. Plus* **130** 97
[11] Salerno M and Kivshar Y S 1994 *Phys. Lett. A* **193** 263
[12] Sen D and Lal S 2000 *Europhys. Lett.* **52** 337
[13] Kundu A 2007 *Phys. Rev. Lett.* **99** 154101
[14] Riazi N and Sheykhi A 2006 *Phys. Rev. D* **74** 025003
[15] Nation P D, Johansson J R, Blencowe M P and Nori F 2012 *Rev. Mod. Phys.* **84** 1
[16] Zhang G F et al 2013 *Chin. Phys. Lett.* **30** 018501
[17] Li H et al 2016 *Chin. Phys. B* **25** 068501
[18] Li G et al 2018 *Chin. Phys. B* **27** 068501
[19] Yang k et al 2018 *Chin. Phys. B* **27** 050701
[20] Li B et al 2018 *Chin. Phys. B* **27** 020701
[21] Nation P D et al 2009 *Phys. Rev. Lett.* **103** 087004
[22] Sabín C 2016 *Phys. Rev. D* **94** 081501
[23] Álvarez L G et al 2015 *Phys. Rev. Lett.* **114** 070502
[24] Marcos D et al 2013 *Phys. Rev. Lett.* **111** 110504
[25] Mezzacapo A et al 2015 *Phys. Rev. Lett.* **115** 240502
[26] Wilson C M et al 2011 *Nature* **479** 376
[27] Lähteenmäki P et al 2013 *Proc. Natl. Acad. Sci. USA* **110** 4234
[28] Lindkvist J et al 2014 *Phys. Rev. A* **90** 052113
[29] Felicetti S et al 2015 *Phys. Rev. B* **92** 064501
[30] Corona-Ugalde P, Martín-Martínez E M, Wilson C M and Mann R B 2016 *Phys. Rev. A* **93** 012519
[31] Lock M P E and Fuentes I 2017 *Time in Physics* chap 5 pp 51–68
[32] Friis N, Lee A R, Truong K, Sabín C, Solano E, Johansson G and Fuentes I 2013 *Phys. Rev. Lett.* **110** 113602
[33] Álvarez L G, Felicetti S, Rico E, Solano E and Sabín C 2017 *Sci. Rep.* **7** 1
[34] Johansson J R, Johansson G, Wilson C M and Nori F 2009 *Phys. Rev. Lett.* **103** 147003
[35] Tian Z H, Jing J L and Dragan A 2017 *Phys. Rev. D* **95** 125003
[36] Makhlin Y, Schön G and Shnirman A 2001 *Rev. Mod. Phys.* **73** 357
[37] You J Q and Nori F 2005 *Phys. Today* **58** 42
[38] Astafiev O, Pashkin Y A, Nakamura Y, Yamamoto T and Tsai J S 2004 *Phys. Rev. Lett.* **93** 267007
[39] Castellanos-Beltran M A and Lehnert K W 2007 *Appl. Phys. Lett.* **91** 083509
[40] Castellanos-Beltran M A, Irwin K D, Hilton G C, Vale L R and Lehnert K W 2008 *Nat. Phys.* **4** 929
[41] Barashenkov I V, Bogdan M M and Korobov V I 1991 *Europhys. Lett.* **15** 113
[42] Braiman Y, Lindner J F and Ditto W L 1995 *Nature* **378** 465
[43] Gavrielides A, Kottos T, Kovanis V and Tsironis G P 1998 *Phys. Rev. E* **58** 5529